Combust. Sci. and Tech., 178: 2199–2218, 2006

ISSN: 0010-2202 print/1563-521X online
DOI: 10.1080/00102200600626108

Taylor & Francis
Taylor & Francis Group

EXPERIMENTAL AND NUMERICAL INVESTIGATION OF TRANSIENT SOOT BUILDUP ON A CYLINDRICAL CONTAINER IMMERSED IN A JET FUEL POOL FIRE

WILLIAM D. CIRO
ERIC G. EDDINGS*
ADEL F. SAROFIM

Department of Chemical Engineering, University of Utah, Salt Lake City, Utah, USA

Soot buildup and its effects on heat transfer have been investigated as part of an effort to understand the thermal response of containers of high-energy materials immersed in fires. Soot deposition rates were measured for cooled and uncooled cylindrical containers immersed in a jet fuel pool fire. The soot buildup was measured at different time intervals with a wet film gage with an uncertainty of 20%. These rates were compared with those calculated by solving the boundary layer equations along the cylinder surface including the thermophoretic transport of soot particles. Thermophoresis was the dominant soot transport mechanism controlling the deposition of soot on the container wall and gave deposition rates in good agreement with the measured values. The soot buildup was found to have an important insulating effect on the heat transfer to the container. A soot deposit thickness of 1.2 mm resulted in as much as a 35% reduction in heat flux.

Received 6 May 2005; accepted 6 February 2006.

This work was sponsored by the Center for the Simulation of Accidental Fires and Explosions at the University of Utah, which was funded by the U.S. Department of Energy under Contract No. LLL B341493, with matching funds provided by the University of Utah Research Fund.

***Address correspondence to eddings@eng.utah.edu**

Keywords: deposition, pool fires, soot buildup, thermal conductivity, thermophoresis

INTRODUCTION

Containers of high-energy materials exposed to an enveloping fire may eventually undergo a thermally induced reaction that can lead to explosions resulting in losses to human life and property. The time to explosion is greatly influenced by the amount of energy reaching the explosive. Estimation of the thermal resistances at the fire/container and container/explosive interfaces is important for obtaining an accurate prediction of time to explosion. This paper focuses on some important issues affecting the fire/container boundary.

The thermal response of objects in fires has been the focus of several studies. Most of them are standard fire tests used by regulatory agencies concerned with transportation of radioactive material containers. According to Longenbaugh (1985), extreme temperature distributions, turbulence, non-homogeneous combustion products, soot particle formation, soot deposition, among others, are some of the factors increasing the complexity of the system. As a result, the object is exposed to a highly absorbing medium and thereby the knowledge of the radiative properties of soot (specially soot absorption coefficient) is crucial for an accurate description of the thermal interactions between the object and the fire. In addition, Gregory et al. (1989) observed that large, cold objects interact and cool the local fire environment and thereby reduce the incoming radiation they receive. Furthermore, the low porosity of soot deposits can act as an additional resistance to the conduction of heat.

Despite the importance of deposition in combustion systems, the factors governing the soot particle transport to "cold" surfaces immersed in flames have not been satisfactorily investigated (Eisner and Rosner, 1985). The deposition may occur by brownian diffusion, inertial impaction, thermophoresis, among others. Rosner and Seshadri (1981), Eisner and Rosner (1985) and Batchelor and Shen (1985) have identified thermophoresis as the dominant process governing deposition of particles in the 10 to 1000 nanometer (nm) diameter size range. This is applicable to combustion systems where the typical diameter range for primary soot particles is 10–100 nm (Makel and Kennedy, 1990).

Makel and Kennedy (1990) reported an experimental and numerical investigation of soot deposition from a hot gas flow to a cooled solid

wall. They used two laser beams at different wavelengths to simultaneously measure soot volume fraction and thickness of the deposited layer. The numerical predictions of soot deposition consisted of solving the boundary layer equations (i.e., momentum, energy and soot transport) on the forward stagnation point of a cylinder in cross flow. The predicted deposition rate agreed very well with the experimental data. Their methodology provides an useful component of a model for calculating the deposition of soot on containers immersed in sooting fires; the extended model must make allowance for the transient nature of the system and the radiative participating properties of soot in the boundary layer and in the deposit.

A reliable prediction of the soot deposit thickness is important for the evaluation of the thermal boundary conditions at the surface of objects engulfed in fires. This paper presents a reliable method for the calculation of transient soot build up on a container immersed in a jet fuel pool fire, validated using a novel soot buildup measuring technique.

EXPERIMENTAL

Cooled and uncooled cylindrical targets were placed 30 cm above the fuel surface of a 30 cm diameter jet fuel pool fire. Yan et al. (2005) present more details on the pool fire facility.

The water-cooled container was made of an 11.43 cm diameter, 10.16 cm long steel pipe (conforming to ASTM A54, 10.16 cm inner diameter). The pipe was divided in two sections, and only the bottom half was used. This configuration has the advantage of allowing a more localized study of the heat flux at the bottom of the container where the deposition is more effective and where the numerical model is applicable. A rotameter and type-K thermocouples were used to measure the flow rate and the inlet and outlet temperatures of the water.

The uncooled container was made of an 11.43 cm diameter, 30.48 cm long steel pipe (conforming to ASTM A54, 10.16 cm inner diameter). 12 type-K thermocouples were fastened to the inner surface of the pipe at different angular locations. The pipe was filled out with a castable refractory material Kastolite 30 that has thermal properties similar to the high-energy material of interest PBX-9501 and therefore represents a surrogate explosive container.

The thickness of the soot buildup was measured with a wet film thickness gauge, which is a metal sheet with a series of notches with

increasing depths (minimum scale of 25 microns). The gauge is placed squarely and firmly onto the container surface to be measured immediately after the fire is extinguished, and then removed. The soot deposit thickness lies between the highest marked notch and the next unmarked notch (for more details see Ciro, 2005, pages 26–27).

For each experiment, the container was cleaned and then suspended by a steel stand such that its bottom surface was approximately 30 cm above the surface of the fuel. Experiments were interrupted at different times to obtain the transient buildup, and each datum point was generated starting with a clean and cold container. In order to determine the bulk density of the soot deposit, samples were carefully removed and the dimensions and weights of each samples were recorded and later used to determine an approximate bulk density.

Gas phase (Oxygen, carbon monoxide and carbon dioxide) and soot particle concentrations were measured at the height of the container following a procedure similar to that of Bouhafid et al. (1989) and Choi et al. (1994), respectively.

The temperature and the velocity of the gases were measured using a pair of fast-response, type-B thermocouples according to the Cross-Correlation Velocimetry CCV technique as presented by Motevally et al. (1992). The method is based on the assumption of a "frozen eddy" that can be traced with the temperature of the fluid particles. The mean velocity is obtained from the measured travel time (i.e., time shift) from one sensor to the second that is located at a known distance downstream of the first.

NUMERICAL STUDY

Deposition Model

Consider combustion gases containing suspended soot particles flowing across a circular cylinder of radius R as shown schematically in Figure 1. The dilute concentration of aerosol particles will not affect the calculated thermophoretic velocity, as explained by Garg and Jayaraj (1990). For low Reynolds number (less than 10^5), the leading half of the cylinder is enveloped by a laminar boundary layer (Zukauskas and Ziugzda, 1985). The velocity and the temperature distributions around the cylinder are therefore governed by the well-known boundary layer equations (White, 1974). For a transient, laminar, two dimensional, incompressible flow, the dimensionless equations are (White, 1974; Garg

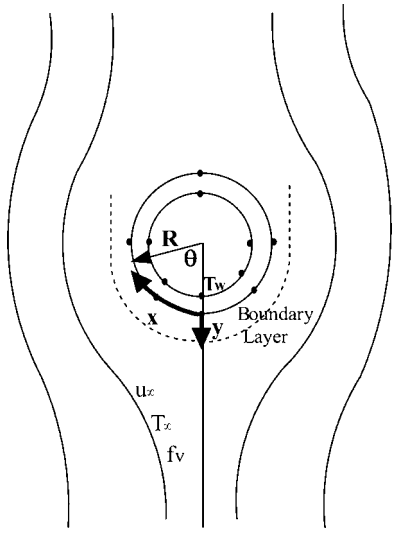

Figure 1. Schematic view of cylinder in cross flow showing relevant variables and coordinate system.

and Jayaraj, 1990; Siegel and Howell, 1992)

$$\frac{\partial U}{\partial X}+\frac{\partial V}{\partial Y}=0 \tag{1}$$

$$\frac{\partial U}{\partial \tau}+U\cdot\frac{\partial U}{\partial X}+V\cdot\frac{\partial U}{\partial Y}=\frac{\partial^2 U}{\partial Y^2}-\frac{dP}{dX} \tag{2}$$

$$\frac{\partial T}{\partial \tau}+U\cdot\frac{\partial T}{\partial X}+V\cdot\frac{\partial T}{\partial Y}=\frac{1}{\mathrm{Pr}}\cdot\frac{\partial^2 T}{\partial Y^2}-\frac{R}{\rho_g\cdot C_p\cdot u_\infty\cdot T_\infty}\cdot\frac{\partial q_r}{dy} \tag{3}$$

where all variables are defined in the Table of Nomenclature.

The local radiative heat flux q_r can be expressed as (Siegel and Howell, 1992)

$$\begin{aligned} q_r(\kappa)=\sigma\cdot T_w^4\cdot\exp\left(-\frac{3}{2}\cdot\kappa\right)-\sigma\cdot T_\infty^4\cdot\exp\left[-\frac{3}{2}\cdot(\kappa_D-\kappa)\right] \\ +\frac{3}{2}\cdot\int_0^{\kappa}\sigma\cdot T_{BL}^4(\kappa')\cdot\exp\left[-\frac{3}{2}\cdot(\kappa-\kappa')\right]\cdot d\kappa' \\ -\frac{3}{2}\cdot\int_{\kappa}^{\kappa_D}\sigma\cdot T_{BL}^4(\kappa')\cdot\exp\left[-\frac{3}{2}\cdot(\kappa'-\kappa)\right]\cdot d\kappa' \end{aligned} \tag{4}$$

The optical path length κ is defined as the integral of the absorption coefficient along the physical path length

$$\kappa = \int_0^y \mathrm{K}_a \cdot dy \tag{5}$$

The net radiative heat flux at the wall of the cylinder can be evaluated as

$$q_{net} = 2 \cdot \sigma \cdot K_a \cdot \int_0^\infty T_{BL}^4 \cdot \exp(-2 \cdot K_a \cdot y) \cdot dy - \sigma \cdot T_w^4 \tag{6}$$

The dimensionless velocity and pressure gradient are found from the potential flow solution over the cylinder

$$U_s = 2 \cdot SIN(X)$$

$$\frac{dP}{dX} = -U_S \cdot \left[\frac{dU_S}{dX}\right] \tag{7}$$

The appropriate boundary conditions for Eqs. (1), (2), and (3) are:

$$U(X,0) = 0;\ U(X,\infty) = U_s(X);\ U(0,Y) = U_s(0);\ V(X,0) = 0$$

$$T(X,\infty) = 1;\ T(0,Y) = 1;\ T(X,0) = \frac{T_w}{T_\infty}$$

According to Wolff et al. (1997), soot particles are convected throughout the core combustion gases by turbulent motion. Since the wall temperature is always less than or equal to the flame temperature, particles passing the boundary layer will experience an average thermophoretic velocity toward the cylinder surface. The mean velocity acquired by the particles relative to the gas is therefore proportional to the temperature gradient (Talbot et al., 1980)

$$V_{th} = -\frac{K_{th}}{T} \cdot \frac{\partial T}{\partial Y} \tag{8}$$

The soot deposit layer thickness can be obtained from the following expression (Makel and Kennedy, 1990)

$$L_{soot} = \rho_{soot} \cdot f_v \cdot V_{th} \cdot \left(\frac{u_\infty}{\mathrm{Re}^{1/2}}\right) \cdot \frac{t}{\rho_d} \tag{9}$$

As the surface temperature increases the deposited soot may oxidize; in this case soot layer thickness can be corrected for oxidation by using

the semi-empirical rate of Nagle and Strickland-Constable (Stanmore et al. 2001).

Soot Effects on Heat Transfer

Duhamel's superposition and inverse heat conduction equations were used to infer the heat flux from the measured temperatures. Beck et al. (1985) presents a detailed description of these methods.

Heat propagates in porous materials mainly by three processes: thermal conduction through the solid phase, radiation, and convection through the pores. Convection can be neglected for small pore sizes and radiation is only important at high temperatures. Therefore, conduction is the dominant energy transport mode in porous combustion systems as concluded by LaVigne et al. (1986) in their numerical and experimental study of deposits in Diesel engine cylinders.

An attempt to quantify the insulating properties of soot deposits requires a good knowledge of the thermophysical properties. The direct measurement of properties such as heat capacity and thermal conductivity is rather complex and expensive. Fortunately, extensive theoretical studies of the thermal properties of porous materials have been made. For instance, according to Litovsky and Shapiro (1992), the effective thermal conductivity for porous materials with a continuous solid phase can be estimated from

$$K_{soot} = K_s \cdot \left[(1-\varepsilon)^{1.5} + \varepsilon^{0.25} \cdot \frac{K_p}{K_s} \right] \tag{10}$$

where K_{soot} is the effective thermal conductivity of the soot layer, K_s is the thermal conductivity of the solid material (assumed to correspond to the experimental values reported for polycrystalline graphite by Pedraza and Klemens, 1993), K_p is the conductivity of the pores and ε is the porosity of the material.

The thermal conductivity of the pore phase has contributions from conduction, convection, radiation and heterogeneous physicochemical processes occurring at the gas-solid interfaces. According to Szelagowski et al. (1999), in most applications, conduction is the dominant contributor to the pore thermal conductivity. In this study, the thermal conductivity of air was utilized for the gas in the pores.

Density and specific heat are also essential to analyze the heat transfer through porous materials. In this work, soot deposit density has been

RESULTS AND DISCUSSION

Experimental Results

The measured fuel flow rate was converted into a mass burning rate by using a density of 800 kg/m^3 and the area of the pool fire. A comparison of the burning rate behavior of Jet A with and without an engulfed container is presented in Figure 3. The reproducibility of the measured burning rate is better than 90%. The transient burning in the early stages is attributed to transient development of flame and temperature distribution in liquid. After approximately 20 minutes, the burning rate is fairly constant and its value is comparable to those reported for jet fuels (Yan et al. 2005). As shown in Figure 3, neither the surrogate explosive nor the water-cooled containers have a significant effect on the burning rate of the fuel. This implies the thermal feedback to the pool from the fire and heat release in the flame were similar in all three cases.

The soot volume fraction at the height of the container averaged a value of 0.83 ± 0.06 ppm (i.e., standard deviation of 8%). The value is in the range reported for jet fuel pool fires (Murphy and Shaddix, 2003). The computed average velocity of the gas was 0.49 ± 0.057 m/s with a 95% confidence level. The flame temperature, after being corrected for radiation cooling ranged between 1150 and 1273 K.

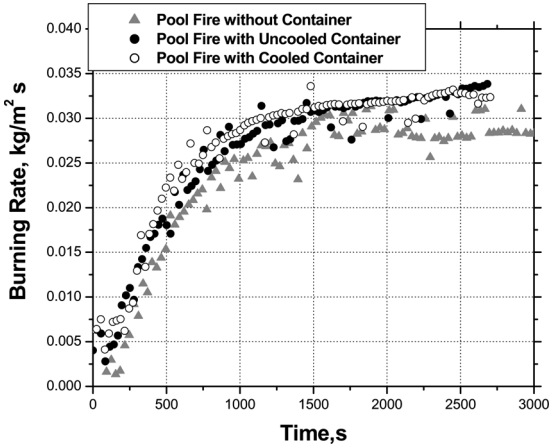

Figure 3. Comparison of experimental burning rates for a 0.3 m-Jet A pool fire with and without engulfing cooled and uncooled cylindrical containers.

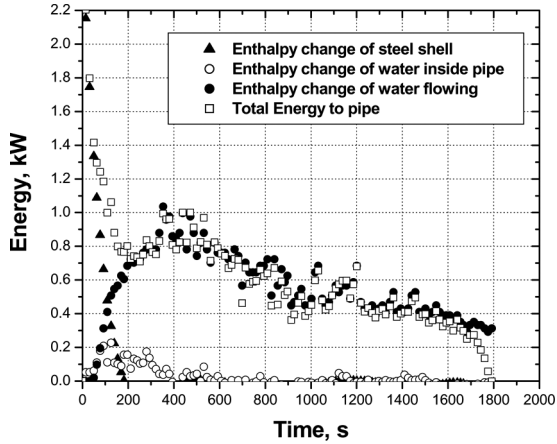

Figure 4. Distribution of total energy to various enthalpy sinks within the pipe calorimeter.

The temperatures at the steel surface and the thermal gradient of the water flowing through the steel pipe (flow rate of 0.061 kg/s) were used in an energy balance on the cooled container (see Eq. 12). As presented in Figure 4, at the early stages of the experiment most of the energy is utilized to heat up the steel shell. After this period, all the energy is effectively absorbed by the water flowing through the pipe. The energy spent in the transient heating of the water of inside the pipe was not important and therefore, the net heat flux to the steel surface is well approximated by the difference in the enthalpy flowing out of and into the pipe. Based on the enthalpy gained by the water, the heat flux at the steel surface[1] is in the range of 50 to 60 kW/m^2 as presented in Figure 5.

The measured inner wall temperature was used to infer the heat flux at the steel and the Kastolite surfaces of the uncooled container. As presented in Figure 6, the net heat flux at the steel surface is about 17 kW/m^2 and decreases with time as a result of a decrease in the thermal driving force (i.e. thermal gradient between the container and the flame decreases), and also due to the insulating effects of soot (i.e., soot may act as a radiation shield in the boundary layer around the container and also as an effective barrier for conduction heat transfer). The net

[1]The thermocouples placed at the inlet and outlet sections of the calorimeter, as well as the top of the calorimeter, were heavily insulated and therefore it is assumed that the area exposed to the fire environment is only the bottom half of the pipe.

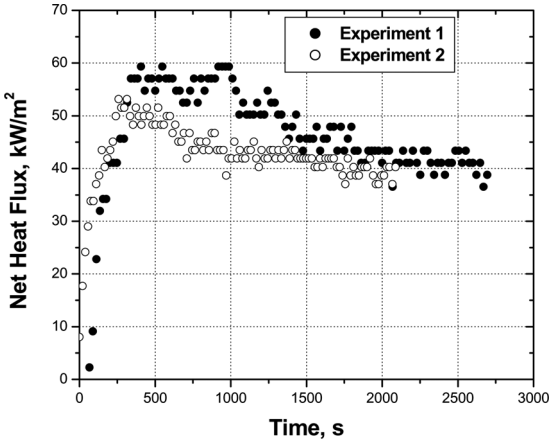

Figure 5. Heat flux at the bottom half of the water-cooled container.

heat flux at the Kastolite surface peaked about 500 seconds after ignition of the fire. The peak heat flux was about 9 kW/m^2, which is only half that at the steel surface. In the early stages most of the heat transfer from the fire is used to heat up the steel shell.

The mean bulk densities of the soot layer were 119 and 35 kg/m^3 for cooled and the uncooled containers respectively. In both cases the

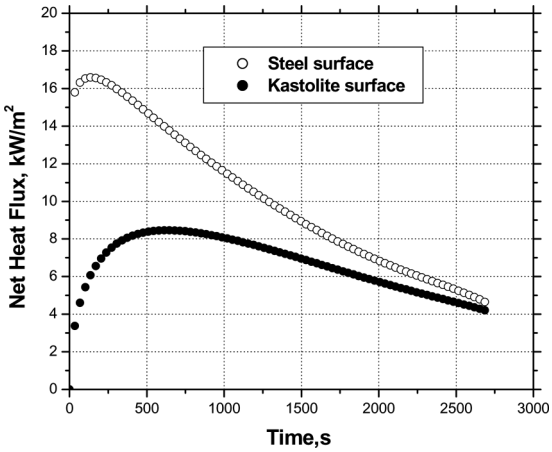

Figure 6. Computed net heat flux at the steel and kastolite surfaces for the uncooled container.

standard deviation was 4% within a confidence level of 95%. A possible reason for this difference is the condensation of polyaromatic hydrocarbons (PAH) on the soot in the cooled boundary layer of the water-cooled container. Such a hypothesis is supported by the observations that (a) soot samples from the cooled container in the present study had a higher PAH content than those from the uncooled container, (b) in an independent study by Smedley et al. (1994) cooled probe soot samples had much larger quantities of PAH than both the uncooled and the free-stream soot samples.

The thermal conductivity of the soot layer was estimated using Eq. (10). The experimental values of thermal conductivity of graphite were taken from Pedraza and Klemens (1993) and were of the same magnitude as those compiled by Goldsmith et al. (1961). The thermal conductivity values of air were adapted from DiNenno et al. (1995). The computed thermal conductivity of the soot layer from the water-cooled container was 3 W/m K. This value was based on an experimental porosity of 90% (determined from the measured bulk density) and an average value of temperature between the container surface and the flame. Equation (10) and an experimental porosity of 97% were used to estimate the thermal conductivity of the soot buildup from the uncooled container. The computed values were found to decrease linearly with temperature according to the formula

$$K_{soot} = 0.97355 - 5.3967E - 4 \cdot T_{soot} \tag{13}$$

Figure 7 presents a comparison of the temperatures at the soot surface and those at the outer and inner walls of the uncooled container (the temperatures at the inner and outer steel walls are indistinguishable). *Soot Surface (Energy Balance)* in Figure 7 was computed according to the energy balance at the soot/steel interface represented by Eq. (11). *Steel outer wall (IHC)* was computed using inverse heat conduction and the measured inner wall temperature, that is *Steel inner wall (Measured)*. The differences in temperature at the soot surface and the outer wall demonstrate the insulating effect of the soot buildup on the surrogate explosive container. Furthermore, the temperature at the soot surface gives a more realistic thermal gradient between the fire and the container, as will be discussed in the next section.

Soot Layer Thickness and Deposition Mechanism

Soot buildup on the bottom of the cylindrical containers was measured with a maximum uncertainty of 20% and confidence level of 95%. The

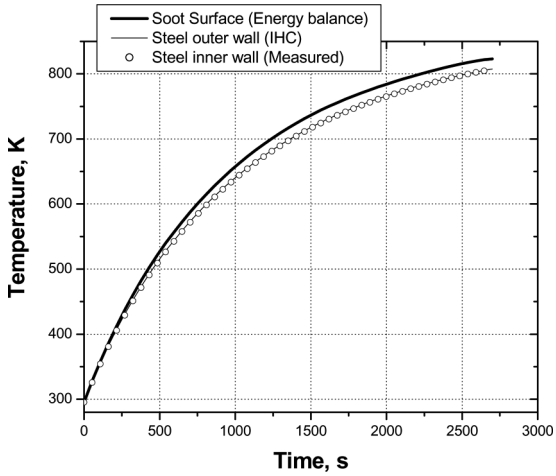

Figure 7. Comparison of temperature at soot surface and at outer and inner walls of the steel pipe of the uncooled container.

deposition model described in the numerical section was used to calculate the soot layer thickness assuming that the deposition occurs only by thermophoresis. Particle deposition by thermophoresis supposes that particles are transported to cold surfaces by means of an existing thermal gradient.

Figure 8 shows that the measured and calculated soot layer thickness on the bottom half of the water-cooled container are in good agreement.

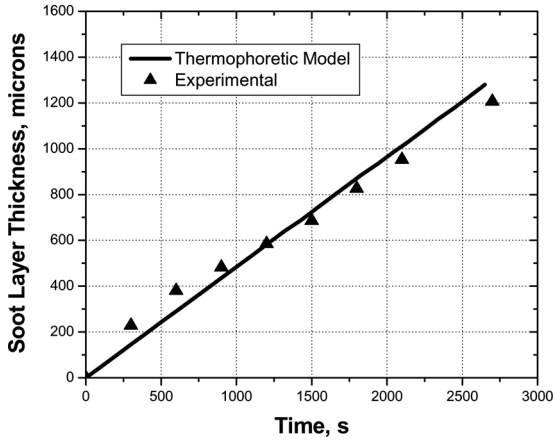

Figure 8. Calculated and measured soot buildup on the surface of a water-cooled container.

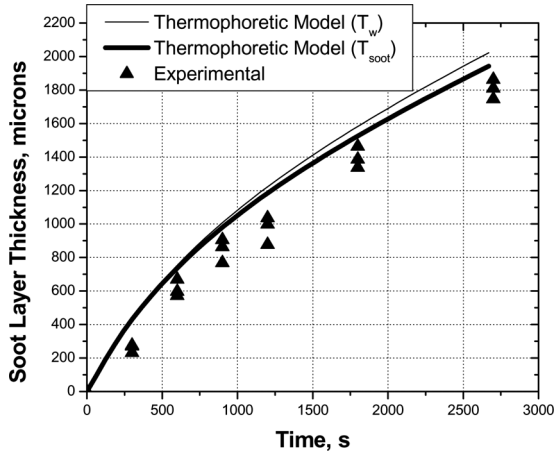

Figure 9. Calculated and measured soot buildup on the surface of the uncooled container.

As expected in the case of constant thermal gradient, the numerical and experimental soot layer thickness increases linearly with time. Thermophoresis is found to be the driving force for soot deposition on a water-cooled container immersed in a jet fuel fire, in good agreement with the results of Makel and Kennedy (1990).

Similarly, Figure 9 presents a comparison of the measured and calculated soot layer thickness on the bottom of the uncooled container (i.e., the forward stagnation point of a cylinder in cross-flow). The use of the steel outer wall temperature (see *Thermophoretic Model* (T_w) in Figure 9) resulted in a slight overestimation of the deposit thickness since the thermophoretic driving force was too large. Better agreement was obtained when the estimated soot surface temperature was used as the boundary condition (see *Thermophoretic Model* (T_{soot}) in Figure 9). Comparisons of the numerical and experimental results suggest a more complex dependence of deposit thickness thermal conductivity with time as a result of variations in deposit temperature, and subsequent variations in deposit conductivity and density.

Soot Insulating Effect

Absorption of radiation by soot in pool fires is important and the knowledge of the radiative properties of soot (i.e., specifically the effective soot

absorption coefficient) is crucial for an accurate description of the thermal boundary condition at the fire/container interface. Typically, researchers have used an absorption coefficient value of 1 m^{-1} (Nicolette and Larson, 1990). According to Koski et al. (1996), the average effective soot absorption coefficient ranged from 0.8 to 2.3 m^{-1} for a JP-4 flame. Longenbaugh (1985) used experimental radiative heat flux measurements inside a sooty pool fire to compute the effective soot absorption coefficient. He reported values that ranged from 0.6 and 1.7 m^{-1}. Souil et al. (1985) reported measurements of soot absorption coefficients in kerosene pool fires. They found values that ranged from 140 m^{-1} near the surface of the fuel to 10 m^{-1} at 50 cm above the fuel surface. These values were measured in the visible region (laser wavelength of 633 nm) and they yielded effective absorption coefficients[2] between 26 and 1.86 m^{-1}. At 30 cm above the fuel surface (this is the height were the container is placed relative to the fuel surface in this work), the effective absorption coefficient was approximately 7.45 m^{-1}. Recently, Murphy and Shaddix (2003) have used a laser transmissivity technique (laser wavelength of 635 nm) to measure the transient soot absorption coefficient in a JP-8 pool fire. The average value they reported was 14 m^{-1}, which yielded an effective absorption coefficient of 2.6 m^{-1}.

Figure 10 presents a comparison of the measured and the computed radiative heat flux at the wall of the water-cooled container. Four cases are presented, (a) *Black body* refers to the net radiative heat flux to a black body; (b) $K_a = 7.45\,m^{-1}$, (c) $K_a = 2.60\,m^{-1}$ and (d) $K_a = 1.00\,m^{-1}$ refer to the average value of the net incident radiative heat flux at the wall computed with absorption coefficients of 7.45, 2.60 and 1.00 m^{-1}, respectively. Their values do not change with time primarily because the model calculations are based on a constant wall temperature. *Experimental* refers to the measured heat flux at the wall of a water-cooled container engulfed

[2]Soot absorption coefficient is usually measured at a wavelength in the visible region of the spectrum. The effective absorption coefficient must account for the dominant contributions in the infrared region. The wavelength $\lambda_{0.5}$ below which half of the blackbody radiation lies is given by $\lambda_{0.5} \cdot T = 4107\,nm\,K$. For $T = 1200\,K$, $\lambda_{0.5} \cong 3400\,nm$. If the absorption coefficient was measured at 633 nm, then the effective absorption coefficient can be calculated as

$$K_{a\_eff} \cong K_a \cdot \frac{633}{3400}$$

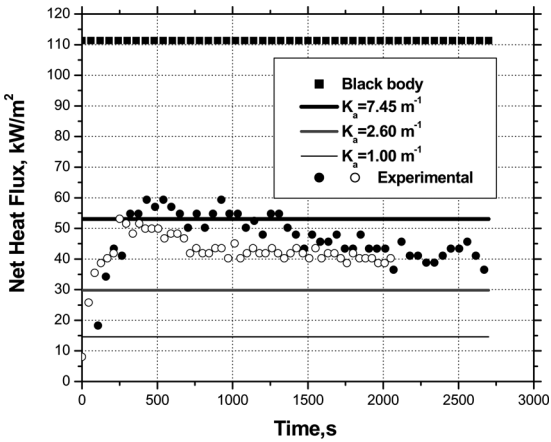

Figure 10. Effects of the absorption coefficient in the net incident heat flux at the wall of a water-cooled calorimeter engulfed by a jet fuel pool fire. The open and closed circles represent two different sets of experimental data for the same conditions.

by a jet fuel pool fire (two different experimental runs are presented in order to show the variability of the data).

The results presented in Figure 10 reveal that the net incident radiative heat flux at the wall for the largest absorption coefficient ($K_a = 7.45\,m^{-1}$, the value measured by Souil et al. (1985) at the same height of the container) was considerably higher than that for the other coefficients ($K_a = 2.6$ and $1\,m^{-1}$) and its value was comparable to that found experimentally. Cold objects receive a much lower heat flux than that from a black body at the gas temperature due to the absorption of soot-laden gases in the fire. For the conditions of the water-cooled container presented in this paper, the heat flux at the wall was only 50% of that of a black body and thus confirms the importance of including the radiative participation of soot and gas in the definition of the appropriate thermal boundary conditions at the fire/container interface.

Regarding the experimental heat flux presented in Figure 10 (i.e., black circles), the first 500 seconds corresponds to the transient start up of the pool fire itself and the heating up of the steel shell. At this time, the heat flux reaches a peak of approximately $60\,kW/m^2$ and then starts decreasing with increasing time as a result of soot building up on the container surface. For the experimental conditions presented in this work (see Figure 8), this reduction in heat flux reaches a value of 35% when the deposit is 1.2 mm thick.

SUMMARY AND CONCLUSIONS

Soot buildup and its effects on heat transfer have been investigated experimentally and numerically as part of an effort to understanding the thermal response of containers of high-energy materials in fires.

The transient soot buildup was measured with a wet film gage, with an uncertainty in the measurement of 20%. This value is comparable to the uncertainty of 15% for laser measurements of soot buildup (Makel and Kennedy, 1990).

Numerical predictions of the transient soot layer thickness were obtained by solving the boundary layer equations and the thermophoretic transport of soot particles to the cylinder surface. The model also considered radiation interactions between soot and gas in the free stream and the cylinder wall. Comparison of the experimental results with the model revealed that thermophoresis appears to govern the deposition of soot on a cylindrical container engulfed in a jet fuel pool fire.

Soot deposited on the surface of the container was found to have an important insulating effect. Although the gas phase species and soot in the flame provide significant absorption of the black body radiation, the soot buildup on the surface of the container was responsible for a considerable reduction in the heat flux. For the conditions of the water-cooled container, this reduction in heat flux became important for a soot layer thickness greater than 0.4 mm and reached a value of 35% when the deposit was 1.2 mm thick.

NOMENCLATURE

A	Area [m^2]
C_p	Heat capacity [J/Kg K]
f_v	Free stream soot volume fraction [ppm(v)]
K	Thermal conductivity [W/mK]
K_a	Soot absorption coefficient [m^{-1}]
K_{th}	Thermophoretic coefficient
L	Thickness [m]
	m_{H2O}
	Mass flow rate of cooling water [Kg/s]
P	Dimensionless pressure
Pr	Prandtl number

q	Heat flux [W/m^2]
q_r	Local radiative heat flux [W/m^2]
q_{net}	Net radiative heat flux at the cylinder wall [W/m^2]
R	Radius of the cylinder [m]
Re	Reynolds number
T	Dimensionless temperature
T_{BL}	Temperature of the gas in the boundary layer [K]
T_{in}	Inlet Temperature of water [K]
T_{out}	Outlet Temperature of water [K]
T_∞	Flame temperature [K]
T_{soot}	Temperature at the soot surface [K]
T_I	Temperature at the soot/steel interface [K]
T_w	Temperature at the container wall [K]
u_∞	Free stream velocity [m/s]
U	Dimensionless velocity component in X direction
U_s	Dimensionless potential flow velocity
V	Dimensionless velocity component in Y direction
V_{th}	Dimensionless thermophoretic velocity
x	Coordinate along the cylinder surface [m]
X	Dimensionless coordinate along the cylinder surface
y	Coordinate normal to the cylinder surface [m]
Y	Dimensionless coordinate normal to the cylinder surface
κ	Optical path length
κ_D	Optical path length to the far field boundary
τ	Dimensionless time
ρ	Density [kg/m^3]
ε	Porosity
σ	Stefan–Boltzmann constant [$= 5.67\ 10^{-8}$ W/m^2 K^4]

Subscripts

∞	Free-stream surroundings
d	Deposit
g	Gas phase
H_2O	Water
p	Porous phase
s	Solid phase
Soot	Soot
Steel	Steel material
w	Wall

REFERENCES

Batchelor, G.K. and Shen, C. (1985) Thermophoretic deposition of particles in gas flowing over cold surfaces. *J. Colloid Interface Sci.*, **107**(1), 21–37.

Beck, J.V., Blackwell, B., and Clair, C.S. (1985) Inverse Heat Conduction: Ill-Posed Problems, John Wiley Interscience Publication, New York, pp. 55–76.

Bouhafid, A., Vantelon, J., and Souil, J. (1989) Characterization of thermal radiation from freely burning oil pool fires. *Fire Safety J.*, **15**, 367–390.

Choi, M., Hamins, A., Rushmeier, H., and Kashiwagi, T. (1994) Simultaneous optical measurement of soot volume fraction, temperature, and CO_2 in heptane pool fire. *Proc. Combust. Instit.*, **25**, 1471–1480.

Ciro, W. (2005) Heat Transfer at Interfaces of a Container of High-Energy Materials Immersed in a Pool Fire, *Ph. D. Dissertation*, University of Utah, Salt Lake City, UT.

Croft, D. and Lilley, D. (1977) Heat Transfer Calculations Using Finite Difference Equations, Applied Science Publishers, London, p. 237.

DiNenno, P. (1995) Appendix B, Property data. In *The SFPE Handbook of Fire Protection Engineering*, National Fire Protection Association, Quincy, MA, A-26.

Eisner, A.D. and Rosner, D.E. (1985) Experimental studies of soot particle thermophoresis in nonisothermal combustion gases using thermocouple response techniques. *Combust. Flame*, **61**, 153–166.

Garg, V.K. and Jayaraj, S. (1990) Thermophoretic deposition over a cylinder. *Inter. J. Eng. Fluid Mech.*, **3**, 175–196.

Goldsmith, A., Waterman, T.E., and Hirschhorn, H.J. (1961) Handbook of Thermophysical Properties of Solid Materials, Rev. ed., Macmillan, New York.

Gregory, J., Keltner, N., and Mata, R. (1989) Thermal measurements in large pool fires. *J. Heat Trans.*, **111**, 446–454.

Koski, J., Gritzo, L., Kent, L., and Wix, S. (1996) Actively cooled calorimeter measurements and environment characterization in a large pool fire. *Fire Mater.*, **20**, 69–78.

LaVigne, P.A., Anderson, C.L., and Prakash, C. (1986) Unsteady Heat Transfer and Fluid Flow in Porous Combustion Chamber Deposits. *SAE Paper No. 860241*, 91–104.

Litovsky, E. and Shapiro, M. (1992) Gas pressure and temperature dependences of thermal conductivity of porous ceramic materials: Part I, refractories and ceramics with porosity below 30%. *J. Am. Ceram. Soc.*, **75**(12), 3425–3439.

Longenbaugh, R.S. (1985) Experimental and Theoretical Analysis of the Radiative Transfer inside of a Sooty Pool Fire. *M.S. Thesis*, Mechanical Engineering, New Mexico State University, Las Cruces, NM, 20.

Makel, D. and Kennedy, I. (1990) Experimental and numerical investigation of soot deposition in laminar stagnation point boundary layers. *Proc. Combust. Instit.*, **23**, 1551–1557.

Motevally, V., Marks, C., and McCaffrey, B. (1992) Cross-correlation velocimetry for measurement of velocity and temperature profiles in low-speed, turbulent, nonisothermal flows. *J. Heat Trans.*, **114**, 331–337.

Murphy, J.J. and Shaddix, C.R. (2003) Soot properties and species measurements in a two-meter diameter JP-8 pool fire. *Sandia National Laboratories Report*, *SAND2003–8246.*

Nicolette, V.F. and Larson, D.W. (1990) The Influence of Large, Cold Objects on Engulfing Fire Environments. *AIAA/ASME Thermophysics and Heat Transfer Conference*, Seattle, WA, 63–70.

Pedraza, D. and Klemens, P. (1993) Effective polycrystalline graphite. *Carbon*, **31**(6), 951–956.

Rosner, D.E. and Seshadri, K. (1981) Experimental and theoretical studies of the laws governing condensate deposition from combustion gases. *Proc. Combust. Instit.*, **18**, 1385–1394.

Siegel, R. and Howell, J. (1992) Chap. 13. The engineering treatment of gas radiation in enclosures. In *Thermal Radiation Heat Transfer*, Hemisphere Publishing Corporation, Washington, DC, pp. 597–678.

Smedley, J., Williams, A., and Mutshimwong, A. (1994) Soot deposition from ethylene/air flames and the role of aromatic intermediates. In Bockhorn, H. (Ed.) *Soot Formation in Combustion: Mechanisms and Models*, Springer-Verlag, Berlin, pp. 403–416.

Souil, J.M., Vantelon, J.P., Joulain, P., and Grosshandler, W.L. (1985) Experimental and theoretical study of thermal radiation from freely burning kerosene pool fires. *10th ICDERS, American Institute of Aeronautics and Astronautics*, 388–401.

Stanmore, B.R., Brilhac, J.F., and Gilot, P. (2001) The oxidation of soot: A review of experiments, mechanisms and models. *Carbon*, **39**, 2247–2268.

Szelagowski, H., Arvanitidis, I., and Seetharaman, S. (1999) Effective thermal conductivity of porous strontiumoxide and strontium carbonate samples. *J. Appl. Phys.*, **85**(1), 193–198.

Talbot, L., Cheng, R., Schefer, R., and Willis, D. (1980) Thermophoresis of particles in a heated boundary layer. *J. Fluid Mech.*, **101**(4), 737–758.

White, F.M. (1974) Viscous Fluid Flow, McGraw-Hill, New York, pp. 241–376.

Wolff, A., Boulouchos, K., and Mueller, R. (1997) A Computational Investigation of Unsteady Heat Flux through an I.C. Engine Wall Including Soot Layer Dynamics. *SAE Paper No. 970063*, pp. 91–104.

Yan, S., Ciro, W., Eddings, E.G., and Sarofim, A. F. (2005) Formulation of a surrogate for the simulation of jet fuel pool fires. *Combust. Sci. Technol.*, **177**(4), 715–739.

Zukauskas, A. and Ziugzda, J. (1985) Heat Transfer of a Cylinder in Crossflow, Springer-Verlag, New York.